

## Original Article

# Assessment of M867, a selective caspase-3 inhibitor, in an orthotopic mouse model for non-small cell lung carcinoma

Bo Li<sup>1</sup>, Justin M Le Blanc<sup>2</sup>, Yunguang Sun<sup>1,2</sup>, Lifeng Yang<sup>2</sup>, Nicholas G Zaorsky<sup>2</sup>, Nicholas J Giacalone<sup>1</sup>, Artour Torossian<sup>1</sup>, Bo Lu<sup>1,2</sup>

<sup>1</sup>Department of Radiation Oncology, Vanderbilt-Ingram Cancer Center, Vanderbilt University School of Medicine, Nashville, TN 37232, USA; <sup>2</sup>Department of Radiation Oncology, Bodine Cancer Center, Thomas Jefferson University School of Medicine, Philadelphia, PA 19107, USA

Received January 2, 2014; Accepted February 6, 2014; Epub March 1, 2014; Published March 15, 2014

**Abstract:** Radiation-induced lung injury (RILI) is a significant dose limiting complication of thoracic radiation for lung, breast, and esophageal cancer. Strategies for increasing the therapeutic index of radiation involve the use of radiosensitizing agents. We investigated the potential of M867 to sensitize non-small cell lung cancer (NSCLC) to radiation *in vivo*, while assessing its protective effects in normal lung parenchyma. H460-Luc2 cells were implanted into the mediastinum of athymic nude mice, which were separated into four treatment groups: control, M867, radiation therapy (RT) or combination. H460-Luc2 cell cultures were treated in parallel. Tumor growth was followed using bioluminescence imaging. Immunohistochemistry staining was used to detect phospho-Smad2/3 and cleaved caspase-3 expression. Western blot was done for the detection of cleaved caspase-3 and phospho-Smad2/3. TUNEL assays were used to measure apoptosis. M867+RT group had significantly increased tumor growth inhibition relative to either treatment alone ( $p=0.02$ ). M867+RT was associated with increased levels of apoptosis ( $p<0.01$ ), but combination treatment was associated with a decrease in caspase-dependent apoptosis relative to RT alone ( $p<0.01$ ). We found that this increase in apoptosis in the M867+RT group was due to caspase-independent cell death. Based on early biomarker analyses of phospho-Smad 2/3 and cleaved caspase-3, M867+RT had a radioprotective effect on normal lung parenchyma. M867 may increase the therapeutic ratio of RT by enhancing the radiosensitivity of NSCLC while mitigating RILI. Further research is warranted to examine the late effects of lung injury and to study differences in the mechanism of action of M867 on lung cancer and normal tissue.

**Keywords:** M867, NSCLC, orthotopic mouse model, caspase, H460-Luc2, radiation

## Introduction

Lung cancer is the most common cause of cancer mortality in the United States and the world, accounting for over 1 million deaths annually [1]. Recent reports by the World Health Organization (WHO) project that lung cancer will occupy sixth place among causes of global mortality by the year 2030 [2]. Preclinical studies utilizing mouse models are an important step in novel drug development for this deadly disease. Most studies utilize an ectopic mouse model for its simplicity and technical feasibility. However, several studies have demonstrated that the unusual microenvironment of such

models may affect outcomes [3-5]. To overcome this limitation, our laboratory recently developed an orthotopic mouse model for locally advanced lung cancer. This model has a low technical barrier, allows non-invasive monitoring of tumor response to treatment, and allows us to monitor radiation-induced-lung-injury (RILI) [6].

Radiation therapy is an important modality in the treatment of lung, breast, and esophageal cancers. However, the dose of thoracic radiation is significantly limited by RILI [7]. One strategy utilized to increase the therapeutic index of radiation therapy (RT) is the administration

## M867 and non-small cell lung carcinoma

of radiosensitizers that promote radiation-induced apoptosis. While caspase inhibitors are believed to inhibit apoptosis, previous studies have reported that the pan-caspase inhibitors, such as ZVAD and Boc-D, may increase apoptosis through unknown caspase-independent mechanisms [8]. In addition, we have shown that a selective caspase-3 inhibitor, M867, enhances the cytotoxic effects of radiation in lung cancer [9]. Thus, M867 has been shown to improve the therapeutic index of radiation.

Many mechanisms and molecules have been reported to induce caspase-independent apoptosis, including Endonuclease G, Omi/htra2, Smac/DIABLO, and apoptosis-inducing factor (AIF) [10]. Notably, each of these pathways has been shown to cause large-scale DNA fragmentation, which appears on terminal deoxynucleotidyl transferase dUTP nick end labeling (TUNEL) assays [11-14]. Additionally, autophagy is a separate and unique mechanism for caspase-independent programmed cell death that does not cause large-scale DNA fragmentation. In autophagy, cytoplasmic constituents are sequestered in autophagosomes (AP), which are then fused with lysosomes to create autolysosomes (ALs), and degraded or recycled. M867 has been shown to be involved in autophagy of H460 cells [9].

RILI is a well-studied phenomenon and the major dose-limiting factor of thoracic radiation. The mechanisms for RILI are complex; however, it is generally believed to be an inflammatory response induced by TGF- $\beta$  and mediated by Smad proteins and caspase-dependent apoptosis [15, 16]. Caspase pathways have also been implicated in inflammatory lung injury secondary to chemotherapy and acute respiratory distress syndrome [17, 18]. The use of caspase inhibitors has been shown to protect from such inflammatory lung injury and remodeling [17-20]. Thus, caspase inhibitors may also have radio-protective effects in RILI.

The effects of M867 have not yet been studied in an orthotopic lung cancer model and our aim was to investigate its ability to sensitize NSCLC to radiation in this microenvironment. In addition, we wanted to study if caspase inhibition with M867 had a protective effect from acute RILI. Our results demonstrate that there is

value in using M867 to sensitize NSCLC to radiation and protect lung parenchyma from RILI.

### Material and methods

#### *Cell line*

H460-Luc2 cells (Caliper Life Sciences) were purchased and re-authentication of the cell lines was not performed because the producer authenticated the cells and they were used less than 6 months after receipt. The cells were maintained in RPMI-1640 culture medium (ATCC), supplemented with 10% fetal bovine serum, and kept at 37°C with humidified 5% CO<sub>2</sub>.

#### *Reagents, antibodies and irradiation*

D-Luciferin Firefly and potassium salt (Gold Biotechnology) were dissolved in DPBS to a final concentration of 15 mg/mL. The solution was filter sterilized through a 0.2  $\mu$ m filter and injected 15 minutes prior to each bioluminescent scan at the dose of 100 mg/kg. M867 (Merck & Co.) was obtained and dissolved in DMSO at a stock concentration of 10 mg/mL. DeadEnd™ Colorimetric TUNEL System kit was purchased from Promega, anti-phospho-Smad2/3 (Ser423/425) was purchased from Santa Cruz Biotechnology, and anti-cleaved caspase 3 were purchased from Cell Signaling Technology. Irradiation was performed using an X-ray irradiator (Therapax, AGFANDT, Inc.).

#### *Tumor cell implantation and tumor growth*

Sixteen female athymic nude mice (nu/nu; each 5 to 6 weeks old) (Harlan Sprague Dawley Inc.) were anesthetized by continuous flow of 2-3% isoflurane; the chest area was sterilized with 70% alcohol pad three times prior to air-drying. Next, 2 x 10<sup>6</sup> H460-Luc2 cells suspended in 100  $\mu$ L of DPBS were injected into the mediastinum. The needle was inserted on the right side of the sternum, midway down, 5 mm in depth, and at a 45° angle with the chest wall. Tumor volume was assessed by bioluminescent imaging (BLI) (Genogen IVIS™ 200 system) starting on day 5. The exposure time was set at 5 seconds for a consistent analysis during follow-up scans. Sixteen mice were recruited to four treatment groups (four mice per group) when tumor growth reached 5 x 10<sup>4</sup> photon counts. A more detailed protocol can be found

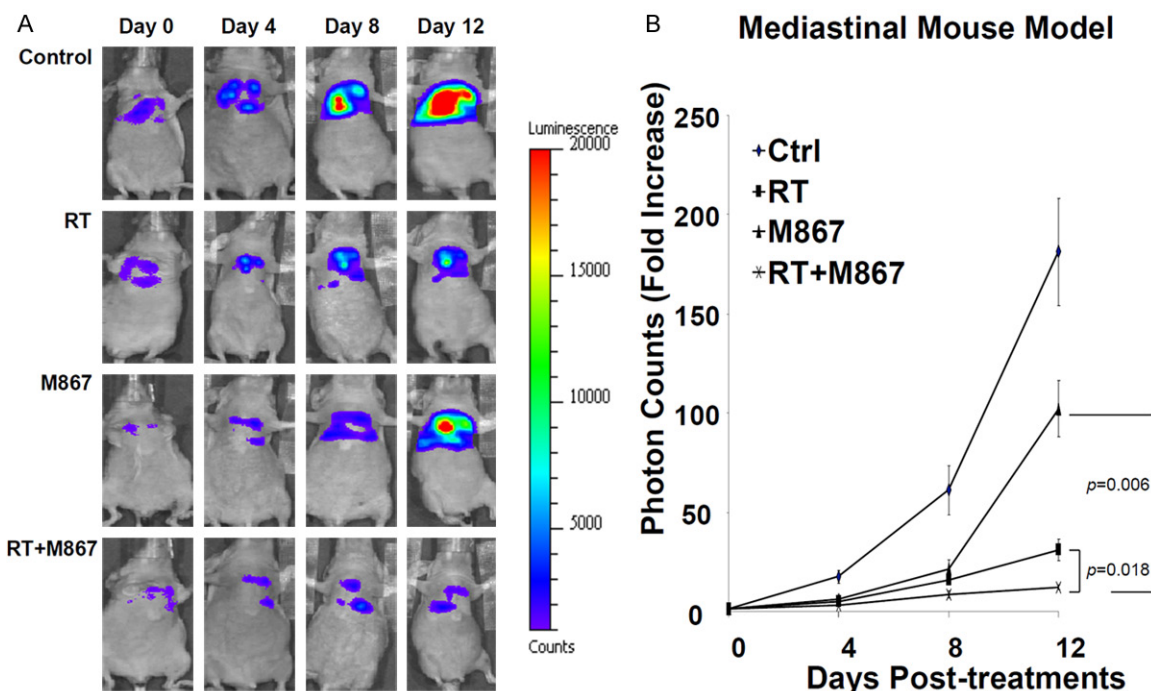


**Figure 1.** M867 Enhances Radiation Induced Tumor Inhibition. A: Mice were separated into 4 groups: DMSO (control), RT (2Gy x 5 days), M867 (2 mg/kg x 7 days), or M867 and RT. First BLI (day 0) was done 2 hours prior to first treatment and repeated every 4 days until day 12. The intensity of BLI is represented by the color. B: Fold increase in BLI was calculated as the proportion of BLI to baseline BLI (day 0). Photon counts of mice from each group were averaged.

in the published mouse model manuscript [6]. Tumor volumes were assessed by BLI every 4 days for a total period of 12 days. Photon counts from the four mice of each group were averaged. Fold increase in BLI was calculated as the proportion of post-treatment BLI to baseline BLI (on first day of treatment).

#### *M867 and radiation treatment of H460-Luc2-implanted mice*

All animal procedures used in this study were approved by the Institutional Animal Care and Use Committee (IACUC) at Vanderbilt University, Protocol #M/08/095. Each group of mice received one of the following treatments: DMSO; RT only; M867 only, M867+RT. All treatments were started on the same day. The RT group received 2 Gy x 5 days. The M867 group received 2 mg/kg x 7 day via intraperitoneal injection. The M867+RT group started with M867 2 mg/kg for 2 days, then RT (2 Gy)+M867 2 mg/kg for 5 days. Radiation was applied to the chests of the mice using an X-ray irradiator; the rest of the body was shielded by lead blocks to avoid radiation.

#### *Immunohistochemistry (IHC)*

One mouse from each treatment group was sacrificed following the last treatment. The mouse lungs and tumors were removed, fixed in 10% formalin for 24 hours and then further processed for immunohistochemical staining. Staining for cleaved caspase-3 and Smad2/3 was performed by Vanderbilt University's IHC core. Briefly, paraffin-embedded tissue slides were de-paraffined with 100% xylene, rehydrated through gradient ethanol series and washed with PBS. The antigen was retrieved by boiling slides in citrate solution for 10 minutes and quenching endogenous horseradish peroxidase (HRP) activity by treating slides with 3% hydrogen peroxide for 30 minutes. Anti-p-Smad2/3 (1:50) was added to sections, slides were placed in a moist container and refrigerated at 4°C overnight. On the next day, slides were washed three times with PBS, and secondary antibody conjugated to HRP (1:200) was added to the section for one hour at room temperature. Slides were then washed with PBS three times and substrate DAB was added to react for 2-5 minutes. Slides were washed

## M867 and non-small cell lung carcinoma

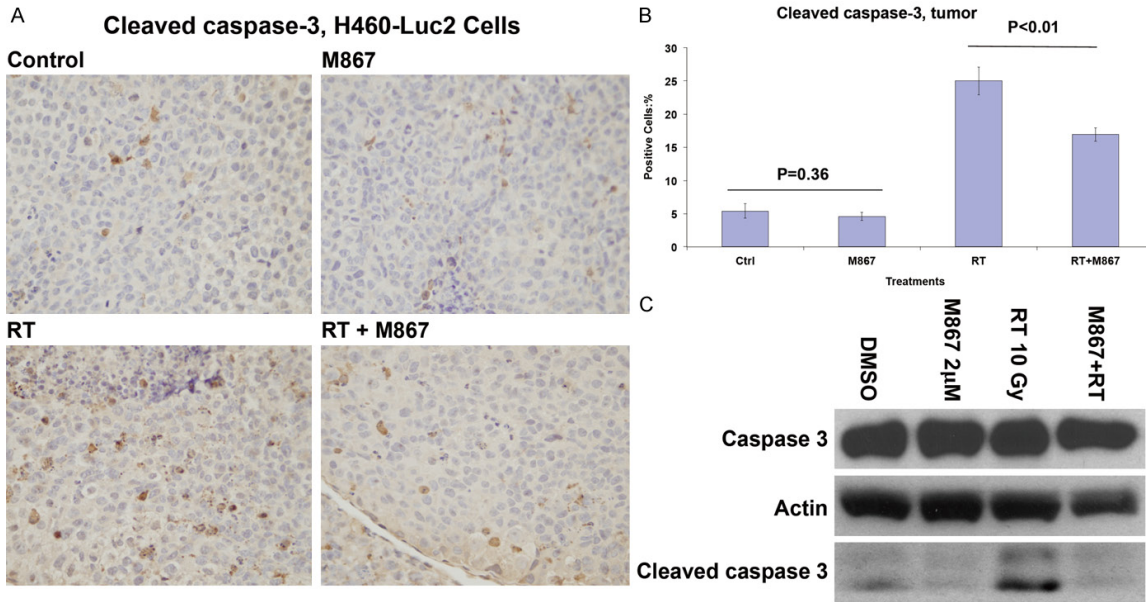


**Figure 2.** M867 Inhibits Radiation Induced, Caspase-3 Mediated Apoptosis. A: One mouse from each treatment group was sacrificed. Tumors of the mice were removed and immunostained for active caspase-3. Shown are representative photographs of histology slides. B: Also shown is a bar graph of mean (10 random fields) percentages of cells that stained positive for active caspase-3 with SEM. *P*-values are indicated. C: Cell cultures (H460-Luc2) were also treated with DMSO, RT (10 Gy), M867 (2  $\mu$ M) or combination. Cells were harvested for protein extraction 48 hours after treatment. Actin was the loading control, Western blots detected cleaved caspase-3.

with water to stop the reaction and counter-stained with hematoxylin for one minute. Slides were dehydrated and mounted with cover slips.

### TUNEL staining

Staining followed procedure provided by manufacturer on both paraffin-embedded tissue slides and live cell cultured slides without modification. The percentage of positive cells was calculated by dividing the number of positive cells by the total cells of each high power field (HPF; 40X magnifications). A total of 10 fields were observed.

### Immunoblotting

H460-Luc2 cells at 80% confluence were treated with DMSO, M867 (2  $\mu$ M), RT (10 Gy), or M867+RT for 48 hours. Cells were harvested for protein extraction and an equal amount of protein was loaded on the 15% SDS-PAGE gel. Proteins were then transferred to the nitrocellulose membrane blot (PerkinElmer Life and Analytical Science), and the blot was incubated with anti-caspase 3 and anti-cleaved caspase-3 antibodies overnight (specific for intact caspase 3 and cleaved caspase-3, respective-

ly). After washing away primary antibody, anti-rabbit secondary antibody was incubated with the blot for one hour. Enhanced chemiluminescence substrate (ECL) (PerkinElmer) was used to detect targeted protein bands.

### Statistical analysis

Data were expressed as mean  $\pm$  standard deviation (SD) or standard error (SE), as indicated. A *p* value of less than 0.05 was considered significant using the *t*-test.

## Results

### M867 enhances radiation-induced tumor growth inhibition

To determine the effect of M867 and radiation on tumor growth inhibition, H460-Luc2-implanted mice were treated with M867 alone, RT alone, M867+RT, or control, and bioluminescent activity was measured. Initial bioluminescent activity in all groups was comparable (not significantly different) at baseline. Mice in the control group had the largest increase in tumor volume with a 180-fold increase relative to baseline (**Figure 1**). M867 alone and RT alone

## M867 and non-small cell lung carcinoma

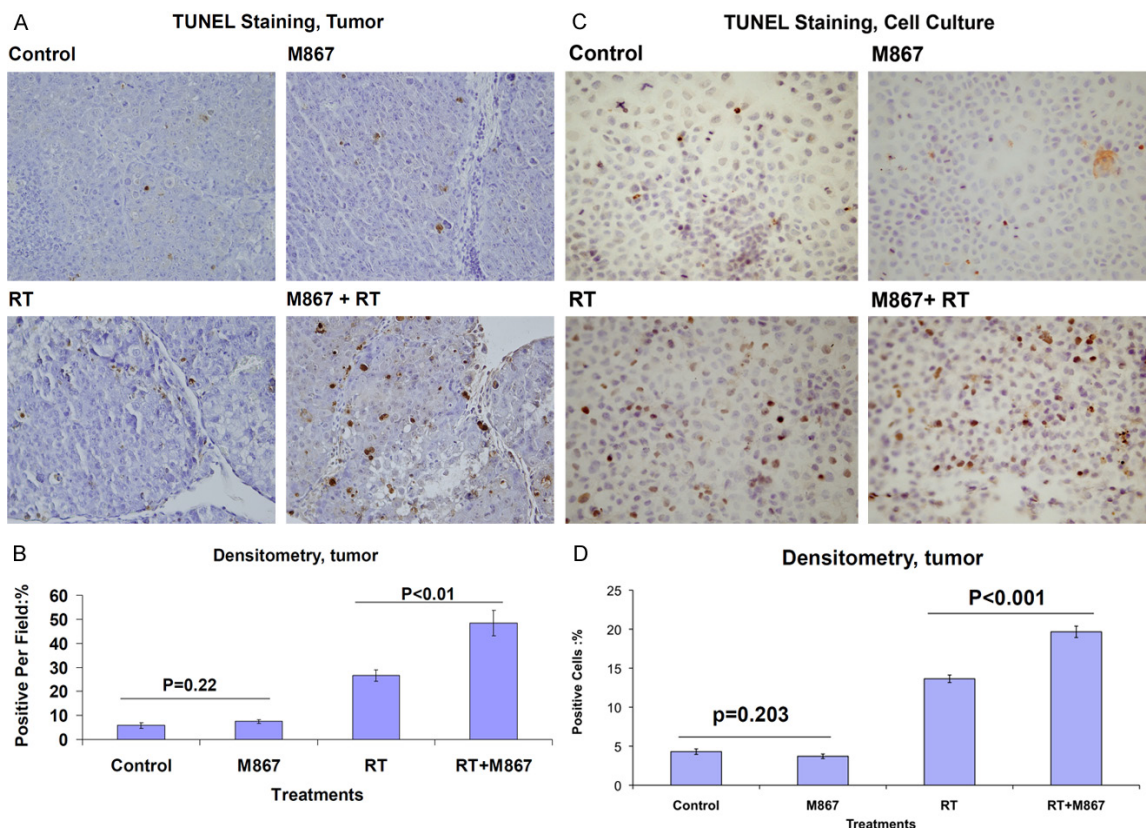


**Figure 3.** M867 Enhances Radiation Induced Apoptosis via a Caspase-Independent Pathway. A: The same tumor tissue slides from **Figure 2** were subjected to TUNEL assay. Shown are representative photographs of histology slides. B: Bar graphs of mean (10 random fields) percentages of cells that stained positive with SEM. *P*-values are indicated. C: Cell cultures (H460-Luc2) were treated with DMSO, RT (10 Gy), M867 (2  $\mu$ M) or combination. Cell culture slides were subjected to TUNEL assay. Shown are representative photographs of histology slides. D: Bar graphs of mean (10 random fields) percentages of cells that stained positive with SEM. *P*-values are indicated.

mice had a 100-fold and 30-fold increase, respectively (Control vs M867 alone,  $p=0.045$ ; Control vs RT alone,  $p=0.001$ ). Combination M867 and RT treatment demonstrated significant tumor inhibition with only a 12-fold photon count increase (Control vs Combination,  $p=0.001$ ; Combination vs M867 alone,  $p=0.006$ ; Combination vs RT alone,  $p=0.018$ ).

### M867 inhibits radiation-induced, caspase-3-mediated apoptosis in lung cancer

To determine the effect of M867 on radiation-induced, caspase-3-mediated apoptosis, one mouse was sacrificed from each treatment group, and IHC was performed for active caspase-3 analysis. Irradiated mice tumors showed increased active caspase-3 staining compared to combination RT and M867 treated mice (25.0% vs. 16.9%, respectively,  $p<0.01$ ; **Figure 2A, 2B**). Tumors of mice treated with

M867 alone did not demonstrate significant differences in cleaved caspase-3 staining from control (4.6% vs. 5.4%, respectively,  $p=0.36$ ; **Figure 2A, 2B**).

This experiment was replicated *in vitro*. H460-Luc2 cell cultures were treated with DMSO, M867 (2  $\mu$ M), RT (10 Gy) or combination M867 and RT (10 Gy). Western Blot revealed that adding M867 to RT effectively inhibited radiation-induced cleaved caspase-3 levels (**Figure 2C**).

### M867 enhances radiation-induced apoptosis via a caspase-independent pathway in tumors

We used TUNEL staining assays to assess total apoptosis in tumor tissues in order to validate the growth inhibition observed in **Figure 1**. Combination treatment resulted in an increased number of DNA fragmentation-dependent apoptotic cells relative to radiation alone (48.4

## M867 and non-small cell lung carcinoma

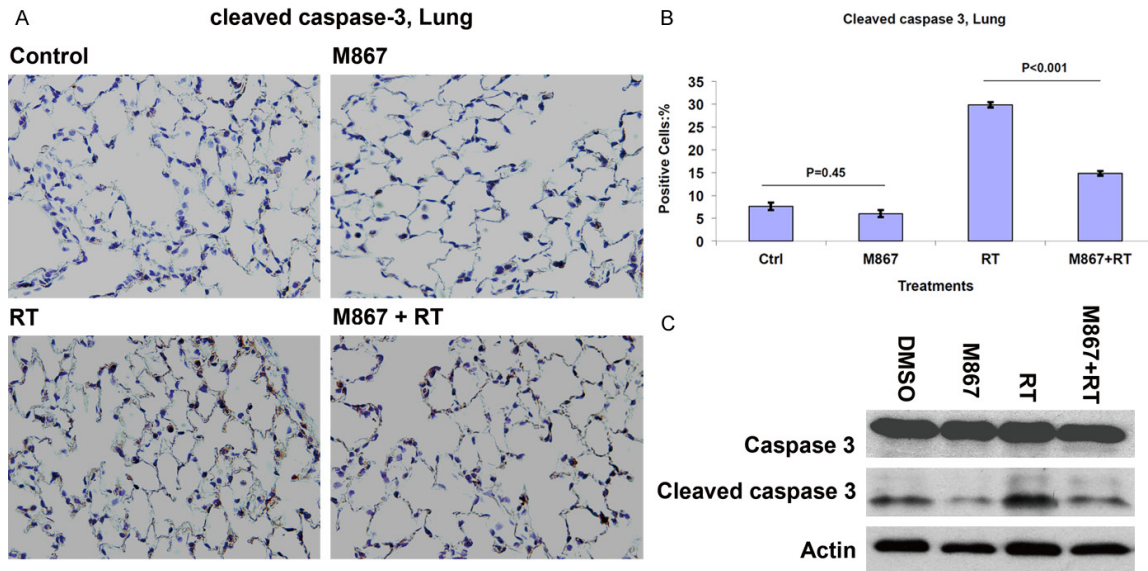


**Figure 4.** M867 Inhibits Radiation Induced, Caspase-3 Mediated Lung Injury. A: One mouse from each treatment group was sacrificed. Mice lungs were removed and immunostained for active caspase-3. Shown are representative photographs of histology slides, magnification is x 40. B: Also shown is a bar graph of mean (10 random fields) percentages of cells that stained positive for active caspase-3 with SEM. P-values are indicated. C: Western blots detected cleaved caspase-3 in protein extracts of mice lungs. Actin was the loading control.

% vs. 26.6%, respectively,  $p < 0.001$ ; **Figure 3A, 3B**). There was no significant difference in observed (per TUNEL assay) apoptotic cells between control and M867 treated mice tumors (**Figure 3A, 3B**).

The experiment was repeated with H460-Luc2 cells *in vitro* with similar results. Combination treatment resulted in an increased percentage of apoptotic cells as compared to radiation alone (19.6% vs. 13.6%, respectively,  $p < 0.001$ ; **Figure 3C, 3D**). There was no significant difference in observed apoptotic cells between control and M867 treated cell cultures (**Figure 3C, 3D**). In order to investigate the mechanism of the caspase-independent apoptosis observed in **Figure 3**, we used densitometry and Western blotting to study the ratio of AIF between the cytoplasm and nucleus. Cell cultures had equal levels of nuclear and cytoplasmic AIF, suggesting that AIF was not involved in M867 enhancement of radiation-induced apoptosis ([Supplemental Figure 1](#)).

### M867 inhibits radiation-induced, caspase-3-mediated lung injury

To determine whether M867 abrogates radiation-induced, caspase-3-mediated lung injury, normal lung tissue was harvested from sacri-

ficed mice, and IHC was performed to measure caspase-3 activation *in vivo*. We found that the cleaved caspase-3 staining densitometry was lower in the combination-treated mouse lung parenchyma relative to RT only treated mice (14.8% vs. 29.8%, respectively; **Figure 4A, 4B**). No difference was observed in cleaved caspase-3 staining between the M867 only and control groups (6% vs. 7.6%, respectively; **Figure 4A, 4B**).

To further validate this finding, Western blotting was used to measure expression of cleaved caspase-3 in treated lung parenchyma. Western blot analysis revealed that the addition of M867 to RT-treated tissue effectively inhibited radiation-induced cleaved caspase-3 levels in mice lung tissue (**Figure 4C**). This confirmed the results observed in **Figure 4A**.

### M867 inhibits radiation-induced apoptosis in lung parenchyma

To elucidate the effect of M867 treatment on radiation-induced apoptosis, TUNEL assays were performed on the lung parenchyma of mice in each of the four treatment groups. RT alone resulted in increased apoptotic cells relative to combination (34.8% vs. 23.7%, respectively,  $p < 0.001$ ; **Figure 5A, 5B**). There was no

## M867 and non-small cell lung carcinoma

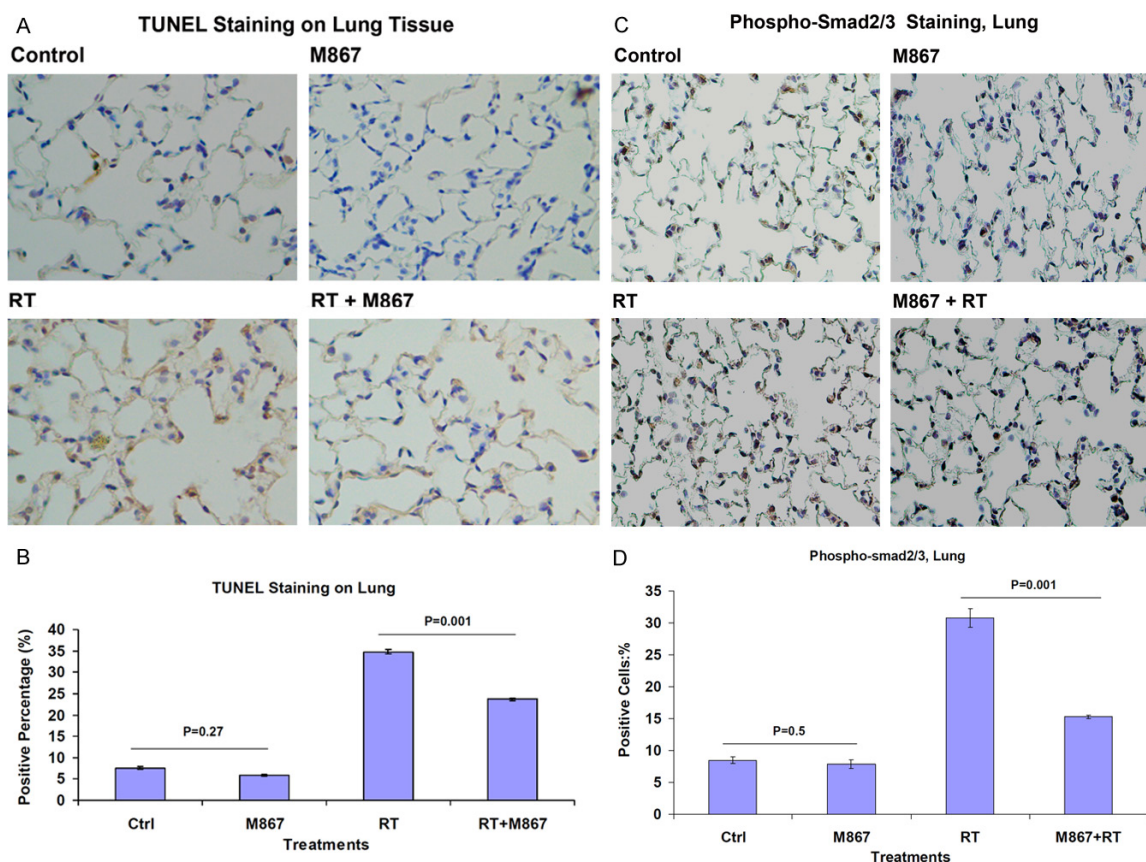


**Figure 5.** M867 Inhibits Radiation Induced Apoptosis and Smad2/3 Mediated Inflammatory Response in Lung Parenchyma. A: Lung tissue slides were subjected to TUNEL assay. Shown are representative photographs of histology slides. B: Bar graphs of mean (10 random fields) percentages of cells that stained positive with SEM. *P*-values are indicated. C: One mouse from each treatment group was sacrificed. Mice lungs were removed and immunostained for p-Smad2/3. Shown are representative photographs of histology slides, magnification is x 40. D: Bar graph of mean (10 random fields) percentages of cells that stained positive for p-Smad2/3 with SEM. *P*-values are indicated.

significant difference in observed apoptotic cells between control and M867 treated mice lung tissue (**Figure 5A, 5B**).

### *M867 inhibits the radiation-induced, Smad2/3-mediated inflammatory response in lung parenchyma*

We used IHC to quantify the treatment effect of M867 on Smad2/3-mediated inflammation in irradiated lung parenchyma. RT only-treated mice lungs showed an increase in phospho-Smad2/3 staining compared to combination RT and M867-treated mice lungs (30.8% vs. 15.2%, respectively,  $p=0.001$ ; **Figure 5C, 5D**). No significant difference in phospho-Smad2/3 staining was observed between M867-treated and DMSO-treated mice lungs (7.8% vs. 8.4%, respectively,  $p=0.5$ ; **Figure 5C, 5D**).

## Discussion

In this study, we showed that M867 enhanced radiation-induced caspase-independent apoptosis in both *in vitro* and *in vivo* settings, and provided a radioprotective effect on healthy lung parenchyma from radiation induced lung injury (RILI). M867 lowered levels of cleaved caspase-3, which is confirmed with previous data showing the caspase 3-inhibitory properties of M867 [9]. Interestingly, TUNEL assays demonstrated increased total apoptosis in lung tumors and decreased total apoptosis in healthy lung tissue when M867 was combined with radiation. These data suggest a role for a caspase-independent apoptotic pathway, in addition to a radioprotective effect in healthy lung tissue.

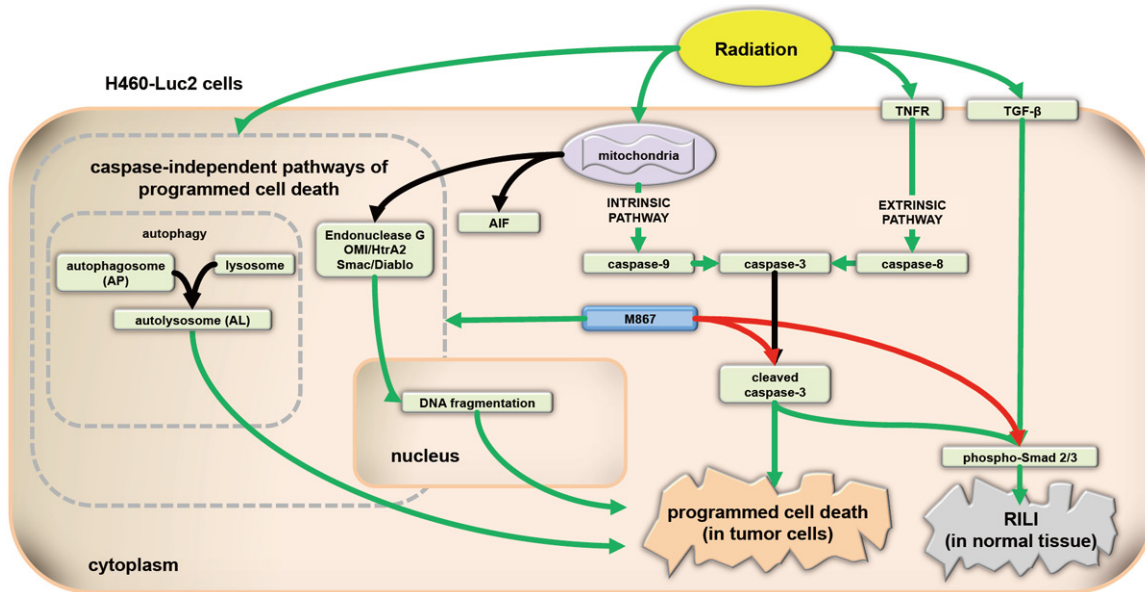


**Figure 6.** Pathways involved in apoptosis and RILI in tumors and normal lung tissue. M867, a selective caspase-3 inhibitor, sensitizes H460-Luc2 NSCLC cells to radiation-induced apoptosis. The effects of M867 are independent of AIF, and may be due to the induction of autophagy. RILI is a significant dose limiting complication of thoracic radiation for lung, breast, and esophageal cancer. Surprisingly, in normal tissue, M867 abrogates RILI, as evidenced by decreased phosphor-Smad2/3 and apoptosis of normal tissue cells.

A recent article by Huang *et al.* suggested that the actions of caspase-3 in tumor cells might be considerably more complicated than previously acknowledged [22]. They suggested that as tumor cells die, they generate and release growth factors, which in turn stimulate the repopulation of cells undergoing radiation treatment. Activated caspase-3 was found to be an important mediator of this process. Xenografts with relatively increased levels of caspase-3 were thus found to be more radiation-resistant due to increased repopulation and not simply intrinsic resistance alone. Similarly, cleaved caspase-3 has also been shown to be a driver for cell migration in ovarian cancer cells [23]. A recent retrospective analysis of patients with head, neck, and breast cancer, who had undergone treatment with radiation, demonstrated that those with increased expression of activated/cleaved caspase-3 had an increased risk for relapse/recurrence and a shorter overall survival [22].

The caspase-dependent apoptotic pathway is a well-established cell death pathway. Caspase-3 and caspase-7 are known to be essential for apoptosis and their inhibition is regarded as a major obstacle to tumor cell death [21]. However, previous studies have demonstrated

the cell death-inducing effects of pan- and specific-caspase inhibitors [8, 9]. Thus, we investigated the effects of M867 in combination with radiation therapy in an orthotopic mouse model. We found that the addition of M867 enhanced cell death and induced apoptosis, while decreasing caspase-3 activation. It was clear that the mechanism of action for the observed apoptosis must be caspase-independent. Since caspase-independent DNA fragmentation was detected on TUNEL assays (Figure 3), autophagy may be the mechanism for caspase-independent, DNA fragmentation-independent, programmed cell death, since apoptosis and DNA fragmentation are closely linked [9] (Figure 6).

In our study, we showed that M867 exerts a strong radioprotective effect on irradiated lung tissue. RILI is a major obstacle to thoracic radiation [7]. RILI is usually an inflammatory reaction that may result in radiation pneumonitis or pulmonary fibrosis [24]. One of the most well studied mediators of lung inflammation and injury is TGF-β. It has been shown to be present extensively in the lungs and regulate inflammation following radiation and chemotherapy [25, 26]. Activated Smad2/3 are well known downstream effectors of TGF-β signaling, thus stain-



ing for phospho-Smad2/3 was chosen as one method of evaluating lung injury [27]. M867 in combination with RT resulted in decreased Smad2/3 levels in lung tissue relative to radiation alone, suggesting decreased inflammation and lung injury. We also used cleaved caspase-3 to evaluate for lung injury, as caspase-3 dependent apoptosis and remodeling, in response to TGF- $\beta$ , has been implicated in long term lung injury [16]. Decreased caspase-3 levels were observed in lung tissue treated with M867 and radiation relative to radiation alone, again suggesting a radioprotective effect of M867 through decreased inflammation, apoptosis, and remodeling in normal lung parenchyma (**Figure 4A, 4B**).

The ability of M867 to radiosensitize lung tumor cells, while providing radioprotective effects on healthy lung parenchyma are ideal properties for an agent to be able to increase the therapeutic index of radiation treatment; however, they are somewhat difficult to explain. One possible explanation is the inherent differences in gene and protein expression profiles between cancerous and normal tissue [10]. Another explanation may be based on the differences in cell turnover and repopulation. As cancer cells have been shown to rely on caspase-3 for repopulation (the “phoenix rising” pathway) [28], M867 may affect their cell turnover in a different method than it does in normal tissue [16, 28]. As discussed in Huang’s and Li’s papers, the “phoenix rising” pathway plays an important role in wound healing and in tumor growth. It remains unclear whether the “phoenix rising” pathway plays a role in the inflammatory response following radiotherapy or in repairing normal lung tissue injury after radiation treatment.

Additionally, it is clear that RILI is a very complex phenomenon that cannot be limited to one single pathway. The limitations of our study are that our orthotopic model has a short lifespan and uses nude (immunocompromised) mice. Therefore, we have to use early markers for radiation-injury (i.e. phospho-Smad 2/3 and cleaved caspase-3), and the model used in this study is only able to provide us with a glimpse of RILI at one point in time. Deciphering the exact mechanism of M867 in tumor and normal lung cells is beyond the scope of this study and will make for an interesting future project.

In conclusion, we have shown the tremendous potential of M867 and other caspase-3 inhibitors in the treatment of NSCLC. We demonstrated that M867 was able to enhance the radiosensitivity of tumors while possibly protecting healthy tissue from RILI, based on the early biomarker (i.e. phospho-Smad 2/3 and cleaved caspase-3) study. As such, M867 could be an ideal agent for increasing the therapeutic ratio of radiation treatment. While further research is warranted to determine the mechanism of action of M867 and other caspase-3 inhibitors on normal vs. cancerous lung tissue, including effects of delayed radiation toxicities (i.e. pneumonitis and pulmonary fibrosis), we believe this class of drugs will one day significantly impact the use of radiotherapy in the clinical setting.

### Acknowledgements

This work was supported by NCI 1R01 CA125842-01A1 (B.L.).

### Disclosure of conflict of interest

None.

**Address correspondence to:** Dr. Bo Lu, Department of Radiation Oncology, Thomas Jefferson University and Hospitals, Inc.G-301 Bodine Cancer Center, 111 S. 11<sup>th</sup> Street Philadelphia, PA 19107. Tel: 215-955-6705; Fax: 215-503-0013; E-mail: bo.lu@jefferson.edu; Bo Li, Department of Radiation Oncology, Vanderbilt-Ingram Cancer Center, Vanderbilt University School of Medicine, Nashville, TN 37232, USA. E-mail: boli6688@gmail.com

### References

- [1] Siegel R, Naishadham D and Jemal A. Cancer statistics, 2012. *CA Cancer J Clin* 2012; 62: 10-29.
- [2] Mathers CD and Loncar D. Projections of global mortality and burden of disease from 2002 to 2030. *PLoS Med* 2006; 3: e442.
- [3] McLemore TL, Liu MC, Blacker PC, Gregg M, Alley MC, Abbott BJ, Shoemaker RH, Bohlman ME, Litterst CC, Hubbard WC, Brennan RH, McMahon JB, Fine DL, Eggleston JC, Mayo JG and Boyd MR. Novel intrapulmonary model for orthotopic propagation of human lung cancers in athymic nude mice. *Cancer Res* 1987; 47: 5132-5140.
- [4] Onn A, Isobe T, Itasaka S, Wu W, O’Reilly MS, Ki Hong W, Fidler IJ and Herbst RS. Development of an orthotopic model to study the biology and

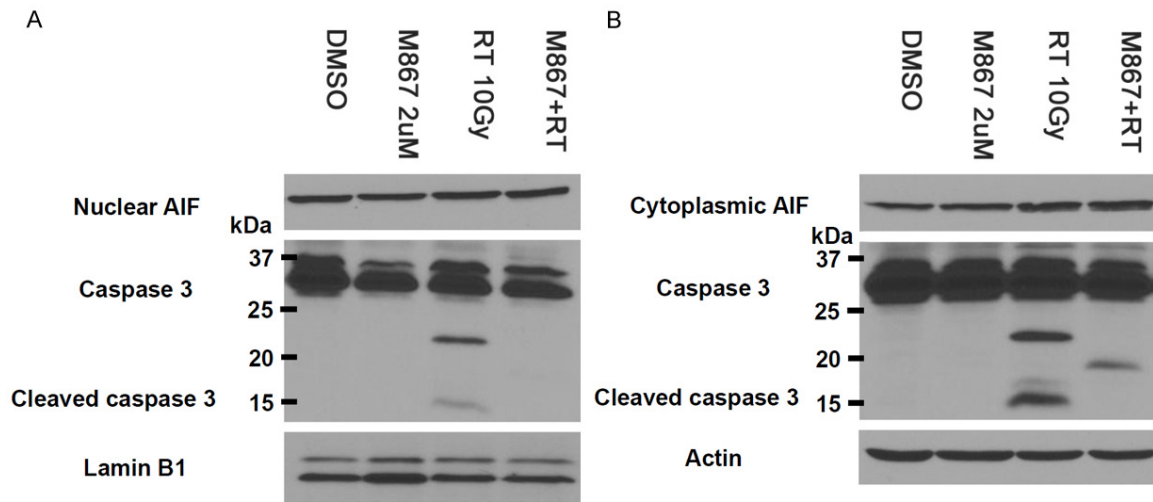
## M867 and non-small cell lung carcinoma

- therapy of primary human lung cancer in nude mice. *Clin Cancer Res* 2003; 9: 5532-5539.
- [5] Killion JJ, Radinsky R and Fidler IJ. Orthotopic models are necessary to predict therapy of transplantable tumors in mice. *Cancer Metastasis Rev* 1998; 17: 279-284.
- [6] Li B, Torossian A, Li W, Schleicher S, Niu K, Giacalone NJ, Kim SJ, Chen H, Gonzalez A, Moretti L and Lu B. A novel bioluminescence orthotopic mouse model for advanced lung cancer. *Radiat Res* 2011; 176: 486-493.
- [7] Madani I, De Ruyck K, Goeminne H, De Neve W, Thierens H and Van Meerbeeck J. Predicting risk of radiation-induced lung injury. *J Thorac Oncol* 2007; 2: 864-874.
- [8] Kim SO, Ono K and Han J. Apoptosis by pan-caspase inhibitors in lipopolysaccharide-activated macrophages. *Am J Physiol Lung Cell Mol Physiol* 2001; 281: L1095-1105.
- [9] Kim KW, Moretti L and Lu B. M867, a novel selective inhibitor of caspase-3 enhances cell death and extends tumor growth delay in irradiated lung cancer models. *PLoS One* 2008; 3: e2275.
- [10] Mathiasen IS and Jaattela M. Triggering caspase-independent cell death to combat cancer. *Trends Mol Med* 2002; 8: 212-220.
- [11] Parrish J, Li L, Klotz K, Ledwich D, Wang X and Xue D. Mitochondrial endonuclease G is important for apoptosis in *C. elegans*. *Nature* 2001; 412: 90-94.
- [12] Su D, Su Z, Wang J, Yang S and Ma J. UCF-101, a novel Omi/HtrA2 inhibitor, protects against cerebral ischemia/reperfusion injury in rats. *Anat Rec (Hoboken)* 2009; 292: 854-861.
- [13] Okada H, Suh WK, Jin J, Woo M, Du C, Ella A, Duncan GS, Wakeham A, Itie A, Lowe SW, Wang X and Mak TW. Generation and characterization of Smac/DIABLO-deficient mice. *Mol Cell Biol* 2002; 22: 3509-3517.
- [14] Lorenzo HK, Susin SA, Penninger J and Kroemer G. Apoptosis inducing factor (AIF): a phylogenetically old, caspase-independent effector of cell death. *Cell Death Differ* 1999; 6: 516-524.
- [15] Flanders KC. Smad3 as a mediator of the fibrotic response. *Int J Exp Pathol* 2004; 85: 47-64.
- [16] Lee CG, Kang HR, Homer RJ, Chupp G and Elias JA. Transgenic modeling of transforming growth factor-beta(1): role of apoptosis in fibrosis and alveolar remodeling. *Proc Am Thorac Soc* 2006; 3: 418-423.
- [17] Kawasaki M, Kuwano K, Hagimoto N, Matsuba T, Kunitake R, Tanaka T, Maeyama T and Hara N. Protection from lethal apoptosis in lipopolysaccharide-induced acute lung injury in mice by a caspase inhibitor. *Am J Pathol* 2000; 157: 597-603.
- [18] Wang R, Ibarra-Sunga O, Verlinski L, Pick R and Uhal BD. Abrogation of bleomycin-induced epithelial apoptosis and lung fibrosis by captopril or by a caspase inhibitor. *Am J Physiol Lung Cell Mol Physiol* 2000; 279: L143-151.
- [19] Kuwano K, Kunitake R, Maeyama T, Hagimoto N, Kawasaki M, Matsuba T, Yoshimi M, Inoshima I, Yoshida K and Hara N. Attenuation of bleomycin-induced pneumopathy in mice by a caspase inhibitor. *Am J Physiol Lung Cell Mol Physiol* 2001; 280: L316-325.
- [20] Kang HR, Cho SJ, Lee CG, Homer RJ and Elias JA. Transforming growth factor (TGF)-beta1 stimulates pulmonary fibrosis and inflammation via a Bax-dependent, bid-activated pathway that involves matrix metalloproteinase-12. *J Biol Chem* 2007; 282: 7723-7732.
- [21] Lakhani SA, Masud A, Kuida K, Porter GA Jr, Booth CJ, Mehal WZ, Inayat I and Flavell RA. Caspases 3 and 7: key mediators of mitochondrial events of apoptosis. *Science* 2006; 311: 847-851.
- [22] Huang Q, Li F, Liu X, Li W, Shi W, Liu FF, O'Sullivan B, He Z, Peng Y, Tan AC, Zhou L, Shen J, Han G, Wang XJ, Thorburn J, Thorburn A, Jimeno A, Raben D, Bedford JS and Li CY. Caspase 3-mediated stimulation of tumor cell repopulation during cancer radiotherapy. *Nat Med* 2011; 17: 860-866.
- [23] Zhao X, Wang D, Zhao Z, Xiao Y, Sengupta S, Xiao Y, Zhang R, Lauber K, Wesselborg S, Feng L, Rose TM, Shen Y, Zhang J, Prestwich G and Xu Y. Caspase-3-dependent activation of calcium-independent phospholipase A2 enhances cell migration in non-apoptotic ovarian cancer cells. *J Biol Chem* 2006; 281: 29357-29368.
- [24] Mehta V. Radiation pneumonitis and pulmonary fibrosis in non-small-cell lung cancer: pulmonary function, prediction, and prevention. *Int J Radiat Oncol Biol Phys* 2005; 63: 5-24.
- [25] Zhao L, Sheldon K, Chen M, Yin MS, Hayman JA, Kalemkerian GP, Arenberg D, Lyons SE, Curtis JL, Davis M, Cease KB, Brenner D, Anscher MS, Lawrence TS and Kong FM. The predictive role of plasma TGF-beta1 during radiation therapy for radiation-induced lung toxicity deserves further study in patients with non-small cell lung cancer. *Lung Cancer* 2008; 59: 232-239.
- [26] Murase T, Anscher MS, Petros WP, Peters WP and Jirtle RL. Changes in plasma transforming growth factor beta in response to high-dose chemotherapy for stage II breast cancer: possible implications for the prevention of hepatic veno-occlusive disease and pulmonary drug toxicity. *Bone Marrow Transplant* 1995; 15: 173-178.
- [27] Kaminska B, Wesolowska A and Danilkiewicz M. TGF beta signalling and its role in tumour

## M867 and non-small cell lung carcinoma

- pathogenesis. *Acta Biochim Pol* 2005; 52: 329-337.
- [28] Li F, Huang Q, Chen J, Peng Y, Roop DR, Bedford JS and Li CY. Apoptotic cells activate the "phoenix rising" pathway to promote wound healing and tissue regeneration. *Sci Signal* 2010; 3: ra13.

### Western blots, tumor



**Supplemental Figure 1.** *AIF Mediates M867 Enhancement of Radiation Induced Apoptosis.* (A and B) H460-Luc2 cell cultures were separated into four groups and given the following treatments: DMSO, 2  $\mu$ M M867, 2Gy RT or M867 and RT for 48 hours. Equal amounts of protein were loaded and run on 12% SDS-PAGE gel. Western blots detected AIF in the cytoplasm and nucleus. Actin (A) and Lamin B1 (B) were the loading controls.